



HAL
open science

The Solar Wind in Time II: 3D stellar wind structure and radio emission

D. Ó Fionnagáin, A.A. Vidotto, P. Petit, C.P. Folsom, S.V. Jeffers, S.C. Marsden, J. Morin, J.-D. Do Nascimento

► **To cite this version:**

D. Ó Fionnagáin, A.A. Vidotto, P. Petit, C.P. Folsom, S.V. Jeffers, et al.. The Solar Wind in Time II: 3D stellar wind structure and radio emission. *Monthly Notices of the Royal Astronomical Society*, 2019, 483, pp.873-886. 10.1093/mnras/stz1308 . hal-01954398

HAL Id: hal-01954398

<https://hal.science/hal-01954398v1>

Submitted on 27 Sep 2024



HAL is a multi-disciplinary open access archive for the deposit and dissemination of scientific research documents, whether they are published or not. The documents may come from teaching and research institutions in France or abroad, or from public or private research centers.

L'archive ouverte pluridisciplinaire **HAL**, est destinée au dépôt et à la diffusion de documents scientifiques de niveau recherche, publiés ou non, émanant des établissements d'enseignement et de recherche français ou étrangers, des laboratoires publics ou privés.



Distributed under a Creative Commons Attribution 4.0 International License

Erratum: The solar wind in time II: 3D stellar wind structure and radio emission

by D. Ó Fionnagáin ¹★, A. A. Vidotto ¹, P. Petit,^{2,3} C. P. Folsom,^{2,3} S. V. Jeffers,⁴ S. C. Marsden,⁵ J. Morin⁶ and J.-D. do Nascimento, Jr.^{7,8}

the BCool Collaboration

¹*School of Physics, Trinity College Dublin, College Green, Dublin 2, Ireland*

²*Université de Toulouse, UPS-OMP, Institut de Recherche en Astrophysique et Planétologie, Toulouse, France*

³*IRAP, Université de Toulouse, CNRS, UPS, CNES, 31400, Toulouse, France*

⁴*Universität Göttingen, Institut für Astrophysik, Friedrich-Hund-Platz 1, 37077 Göttingen, Germany*

⁵*University of Southern Queensland, Centre for Astrophysics, Toowoomba, QLD, 4350, Australia*

⁶*Laboratoire Univers et Particules de Montpellier, Université de Montpellier, CNRS, F-34095, France*

⁷*Departamento de Física, Universidade Federal do Rio Grande do Norte, CEP: 59072-970 Natal, RN, Brazil*

⁸*Harvard-Smithsonian Center for Astrophysics, Cambridge, MA 02138, USA*

Key words: errata, addenda – stars: winds, outflows – stars: solar-type – radio continuum: stars.

This is an erratum to the paper ‘The solar wind in time - II: 3D stellar wind structure and radio emission’, which was published in MNRAS, 483(1), 873, 2019 (Ó Fionnagáin et al. 2019). In Section 4.1, ‘Radiative transfer model’, we outline the calculations to determine radio emission from the stellar winds simulated earlier in the work. Equation (16) defines the absorption coefficient of the plasma. While this equation is correct, there was a typo in the radiowinds code. In our simulations $n_i = n_e = n/2$ and $n^2 = n_i^2/4$, however in the code to calculate absorption coefficients this was written as $n^2 = (n_i/4)^2$, giving absorption coefficients 4 times smaller than anticipated. The typo in the radiowinds¹ python module has been rectified.

This has the effect of increasing radio fluxes from these stellar winds by a factor of 4, which does not effect the scientific results of the paper, and in fact, further supports the discussion made in Section 5. Due to the factor of 4 increase in predicted stellar wind fluxes, the following numbers should be updated in the text:

(i) the radio flux density of κ^1 Cet quoted in Section 4.2, the Abstract and Section 5 should change from 0.73 μJy to 2.83 μJy .

(ii) the radio flux density of χ^1 Ori quoted in Section 4.2 and conclusion should be updated from 2.2 μJy to 8.3 μJy . This is only a factor of 10 smaller than the upper limits set by Fichtinger et al. (2017). Emission at 100 μJy would require a base density only three

times larger ($\approx 6 \times 10^9 \text{ cm}^{-3}$ instead of the quoted $\approx 10^{10} \text{ cm}^{-3}$) than base densities we used in our work. From this we can derive that the mass-loss rate of χ^1 Ori is no larger than $1.4 \times 10^{-11} M_\odot \text{ yr}^{-1}$ instead of the quoted value, $2 - 3 \times 10^{-11} M_\odot \text{ yr}^{-1}$.

(iii) Changes to radio flux density calculations for other stellar winds are updated in Table 2.

Although our updated values do not change the main conclusion of our paper, the detectability of these winds looks more promising (see Fig. 8a):

(i) χ^1 Ori is now partially detectable by VLA at frequencies between 1 and 2 GHz, ignoring other sources of emission.

(ii) Both optically thick and thin regimes of χ^1 Ori and κ^1 Cet should be readily detectable by SKA1-MID.

(iii) The optically thin regimes of all other stars in the sample should be detectable by SKA2-MID, with the optically thick regimes possibly detectable for HD 190771, HD 76151, and 18 Sco.

(iv) The coefficient and power index for equation (21) have been updated to reflect the updated flux densities.

$$S_{\nu, 1\text{GHz}} = 0.68 \left[\frac{\Omega}{\Omega_\odot} \right]^{0.7} \left[\frac{10\text{pc}}{d} \right]^2 \mu\text{Jy} \quad (21)$$

The updated figures and tables are shown below. We thank Robert Kavanagh for bringing this typo to our attention.

* E-mail: ofionnad@tcd.ie

¹radiowinds is available at github.com/ofionnad/radiowinds

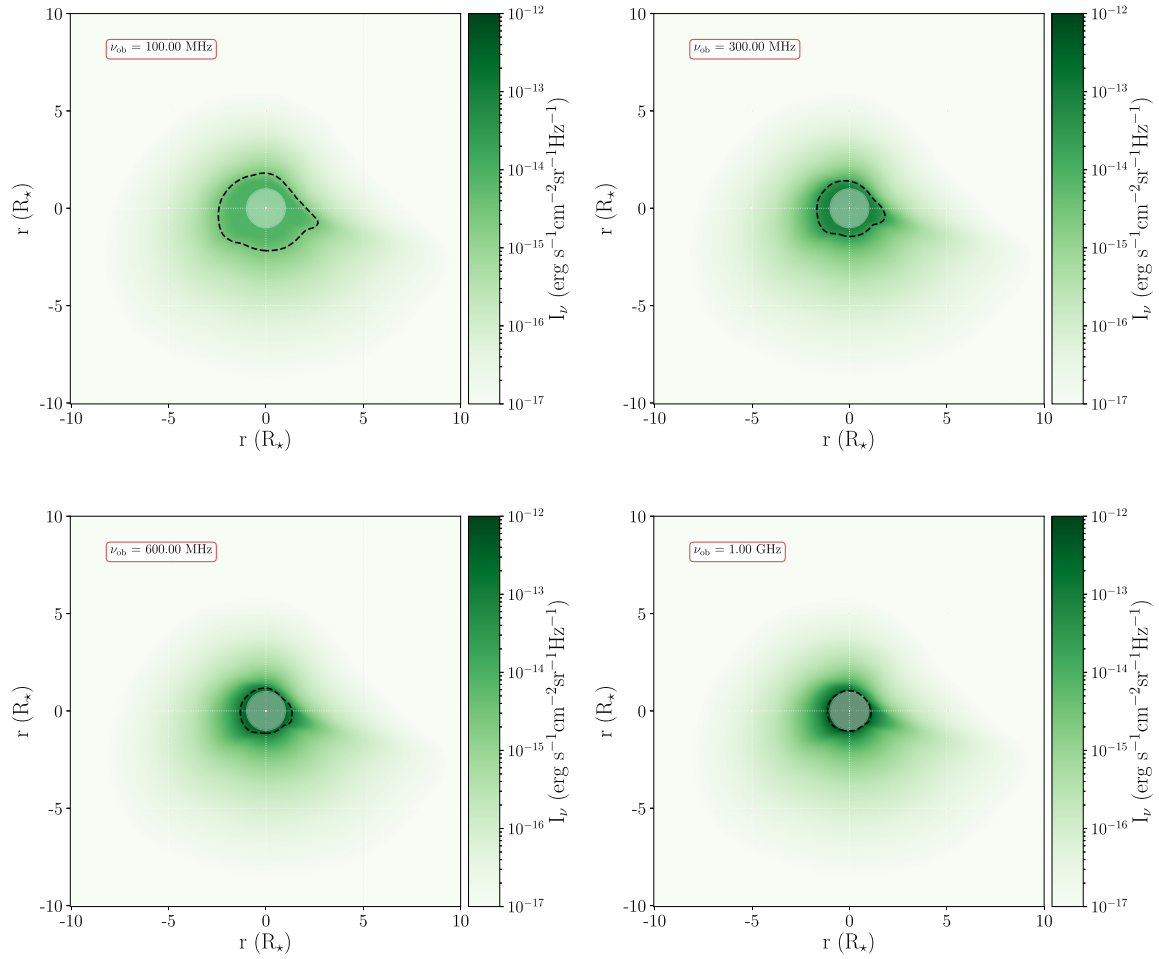
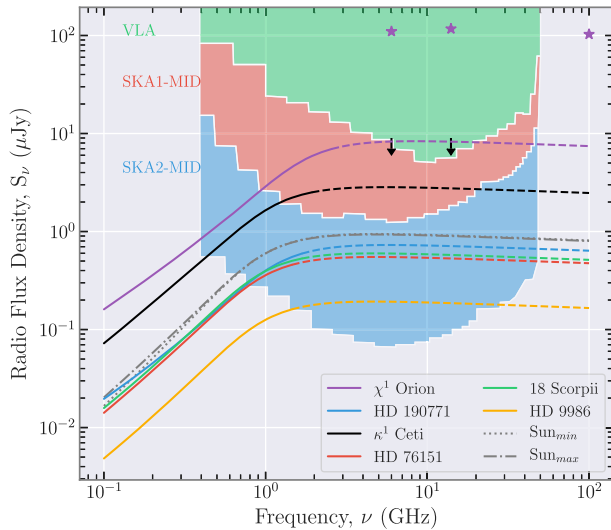
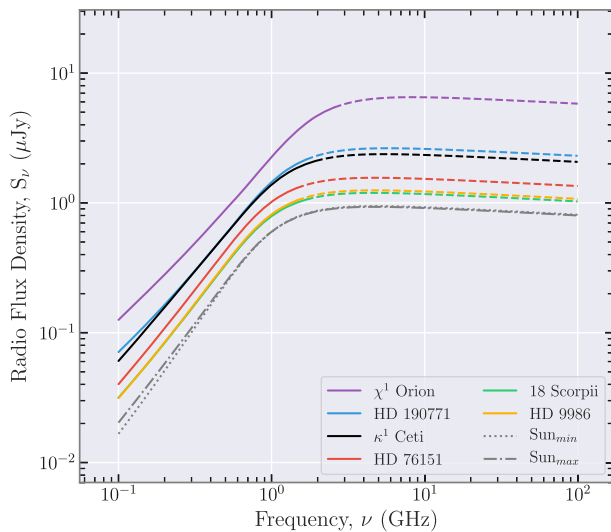


Figure 7. Example of intensity and optical depth for κ^1 Ceti at observing frequencies of 100 MHz (top left), 300 MHz (top right), 600 MHz (bottom left) and 1 GHz (bottom right). The green colour scale represents the intensity of emission from the wind, looking along the line-of-sight of our simulation grid. The dashed black contour represents the region where the wind becomes optically thick, according to Panagia & Felli (1975), $\tau = 0.39$). We can see that the emission is anisotropic due to the anisotropy of the wind density and temperature. The intensity reaches a maximum in the thin regime, as we can see emission from the entire wind. The white circle denotes $R = 1 R_*$. Plasma in front of the star still emits in radio, but we have excluded any contribution from behind the star along the line-of-sight.



(a)



(b)

Figure 8. *Top:* We see that the radio spectra for each wind are very similar in shape. Differences in flux density are strongly affected by distance to the object. The dashed lines represent the optically thin part of each spectrum, and there are differences in where the emission becomes optically thin from star to star at the frequency ν_{thin} . The black arrows indicate the observational upper limits of κ^1 Ceti found by Fichtinger et al. (2017). From the same work we mark the chromospheric detections of χ^1 Ori (purple stars), using both VLA and ALMA, which is concluded to originate from chromospheric emission. Our results show this conclusion to be valid as we predict the wind to emit at much lower fluxes. Sensitivities of the current VLA and future SKA1-MID and SKA2-MID are included shaded in green, red, and blue respectively (SKA sensitivities from Pope et al. 2019 and adjusted for 2 hour integration time). *Bottom:* Here we normalised spectra in the top panel to a distance of 10 pc. This allows direct comparison of radio emission to an ageing solar wind. As the stars age and spin-down the radio emission decreases by an order of magnitude between 500 Myr and 4.6 Gyr.

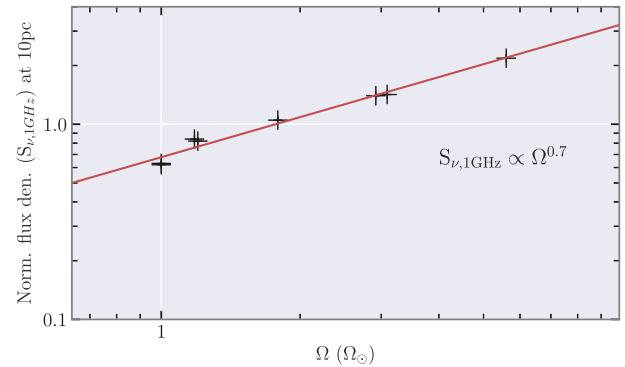


Figure 9. Normalised flux density at 1 GHz as a function of stellar rotation. We see a tight fit to this power-law (see equation 21), with an almost linear dependence of stellar wind radio flux on stellar rotation at 1 GHz.

Table 2. Predicted radio emission from our stellar wind models. Example fluxes at a frequency of 6 GHz are given ($S_{6\text{GHz}}$), in this case we find that all of the winds would be optically thin at this frequency. The power law fit to the spectra was conducted between 0.1 and 1 GHz, giving the coefficient (S_0) and power index (ϕ). However, the spectral slope between these two frequencies varies substantially, tending to shallower slopes at higher frequencies. Depending on the fitting range, slopes can range from 0.6 to 1.5. All slopes tend to -0.1 in the thin regime. The final column gives the frequency at which each wind becomes optically thin (ν_{thin}).

Star	$S_{6\text{GHz}}$ (μJy)	S_0	ϕ	ν_{thin} (GHz)
χ^1 Ori	8.28	2.78	1.26	2.80
HD 190771	0.73	0.39	1.32	1.85
κ^1 Ceti	2.83	1.67	1.35	2.13
HD 76151	0.55	0.37	1.41	1.61
18 Sco	0.60	0.40	1.40	1.63
HD 9986	0.19	0.13	1.42	1.63
Sun max (10 pc)	0.94	0.63	1.55	2.01
Sun min (10 pc)	0.93	0.62	1.47	2.00

REFERENCES

- Fichtinger B., Güdel M., Mutel R. L., Hallinan G., Gaidos E., Skinner S. L., Lynch C., Gayley K. G., 2017, *A&A*, 599, A127
 Ó Fionnagáin D. et al., 2019, *MNRAS*, 483, 873
 Panagia N., Felli M., 1975, *A&A*, 39, 1
 Pope B. J. S., Withers P., Callingham J. R., Vogt M. F., 2019, *MNRAS*, 484, 648

This paper has been typeset from a $\text{\TeX}/\text{\LaTeX}$ file prepared by the author.